Thermodynamic properties and phase equilibria of branched chain fluids using first- and second-order Wertheim's thermodynamic perturbation theory

Felipe J. Blas
Departamento de Física Aplicada e Ingeniería Eléctrica, Escuela Politécnica Superior, Universidad de Huelva, 21819 La Rábida, Huelva, Spain, and Departament d'Enginyeria Química, ETSEQ, Universitat Rovira i Virgili, Carretera de Salou s/n, 43006 Tarragona, Spain

Lourdes F. Vega[a)]
Departament d'Enginyeria Química, ETSEQ, Universitat Rovira i Virgili, Carretera de Salou s/n, 43006 Tarragona, Spain

(Received 20 March 2001; accepted 6 June 2001)

We present an extension of the statistical associating fluid theory (SAFT) for branched chain molecules using Wertheim's first- and second-order thermodynamic perturbation theory with a hard-sphere reference fluid (SAFT-B). Molecules are formed by hard spherical sites which are tangentially bonded. Linear chains are described as freely jointed monomeric units, whereas branched molecules are modeled as chains with a different number of articulation points, each of them formed by three arms. In order to calculate the vapor–liquid equilibria of the system, we have considered attractive interactions between the segments forming the chain at the mean-field level of van der Waals. The Helmholtz free energy due to the formation of the chain is explicitly separated into two contributions, one accounting for the formation of the articulation tetramer, and a second one due to the formation of the chain arms. The first term is described by the second-order perturbation theory of Phan *et al.* [J. Chem. Phys. **99**, 5326 (1993)], which has been proven to predict the thermodynamic properties of linear chain fluids in a similar manner to Wertheim's approach. The formation of the chain arms is calculated at Wertheim's first-order perturbation level. The theory is used to study the effect of the chain architecture on the thermodynamic properties and phase equilibria of chain molecules. The equation predicts the general trends of the compressibility factor and vapor–liquid coexistence curve of the system with the branching degree, in qualitative agreement with molecular simulation results for similar models. Finally, SAFT-B is applied to predict the critical properties of selected light alkanes in order to assess the accuracy of the theory. Experimental trends of the critical temperature of branched alkanes are qualitatively captured by this simple theory. © *2001 American Institute of Physics.* [DOI: 10.1063/1.1388544]

I. INTRODUCTION

Great effort has been made in recent years toward the development and use of accurate equations of state for the determination of the thermodynamic properties and phase equilibria of fluids in general, and chainlike systems in particular (see the book of Sengers *et al.*[1] for a recent review). Most of the processes used in the chemical and oil industries involve nonspherical molecules, such as light and heavy hydrocarbons, and polymers. A great advance in this field has been made by the use of modern molecular theories, which provide a realistic description of the free energy of the system, as they are able to make quantitative predictions for the phase behavior of complex systems. However, an accurate molecular description of the thermodynamic behavior and phase equilibria of branched chainlike molecules is less common. This kind of substance is frequently used in the chemical process design and chemical industries. Applications include their use as solvents for supercritical extraction purposes and in general, as new components for separation and extraction operations. Branched chainlike molecules are also important components in polymeric blends, which can determine some specific and desired thermodynamic properties.

Numerous molecular-based theories have been proposed in recent years to predict the thermodynamic properties and phase equilibria of nonspherical molecules. Among them, the most popular approaches are the reference interaction site model (RISM),[2,3] its extension to deal with polymers (PRISM),[4–7] the perturbated hard chain theory,[8] the generalized-Flory theories,[9,10] the Percus–Yevick theory based chain equation of state,[11] and Wertheim's first-order thermodynamic perturbation theory (TPT1).[12,13] Most of these theories have been used to study the thermodynamic properties of linear chain fluids, although some attempts to predict the behavior of branched systems have also been made. Yethiraj and Hall[14] have performed molecular simulations to obtain the thermodynamic properties of branched hard chains, and results have been compared with the predictions from the generalized-Flory dimer equation of state.[10]

[a)]Author to whom correspondence should be addressed. Electronic-mail: lvega@etseq.urv.es

More recently, Escobedo and de Pablo[15] have presented a novel approach which combines the generalized-Flory theory, the Wertheim approach, and computer simulation to predict the thermodynamic properties of branched hard chain systems.

The SAFT approach,[16,17] based on Wertheim's first-order perturbation theory,[12,13] is an equation originally developed for associating fluids. One can use it for making chain molecules having a spherical reference fluid, with the appropriate number of associating sites and the right stoichiometry, and taking the limit of full association.[18,19] This theory has been widely used to predict thermodynamic properties and phase behavior of linear chain molecules.[20–37]

Most versions of the SAFT equation of state are based on TPT1.[12,13] At this level of approximation, the Helmholtz free energy due to the formation of the chain depends only on the number of segments forming the molecules, but not on how the beads are connected to make up the chain; only contributions containing one associating bond are considered in the evaluation of the Helmholtz free energy, which are embedded in the term involving the pair radial distribution function of the reference fluid. This implies that the bond formation is assumed to be independent of each other, and that the overall effect of bonding is approximated by the formation of one bond multiplied by the total number of bonds in the chain fluid. This is a good approximation for linear chains, in which all the connections between segments can be considered as equivalent along the chain molecule. However, this is no longer true for the case of branched chains, since the articulation segments and those connected to it behave in a different way than the segments located in the chain arms.

Wertheim's second-order perturbation theory (TPT2)[13] accounts, explicitly, for the correlation between three consecutive beads, describing in a more accurate way how the segments are arranged along the chain. It is always possible to obtain a more reliable description of the Helmholtz free energy using the formalism of Wertheim at higher orders of the perturbation scheme, but the structural information needed for this is not readily available. There have been several works published in recent years using the second-order perturbation theory to account for the formation of the chain. In particular, Müller and Gubbins[38] have studied the thermodynamic and structural properties of hard triatomic and tetratomic fluids using molecular simulation and the theory of Wertheim at the second-order level. Agreement between theoretical predictions and simulation data is remarkable in most cases, but the theory was not extended for longer chains. Phan *et al.*[39] have derived a new version of the TPT2 using the formalism of Wertheim within the framework of monodisperse polymerization, in contrast with the approaches of Wertheim and Müller and Gubbins, which are based on a reference polydisperse mixture. Although the resulting equations have different analytical expressions, Phan *et al.*[39] have demonstrated that predictions by the two versions of the theory are very similar. These authors have also proposed a general framework for developing equations of state for starlike molecules, although the calculation of the Helmholtz free energy due to the formation of the chain is rather tedious. More recently, Shukla and Chapman[40] have presented the extension of the TPT2 equation of state to deal with mixtures consisting of linear heteronuclear hard chain molecules. In all cases, the TPT2 predictions provide a more accurate description than the TPT1 version of the theory, as expected.

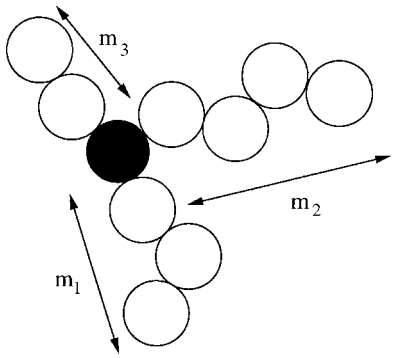

FIG. 1. Two-dimensional view of the molecular model for branched chains with three arms (blank segments) and one articulation point (dark segment). The articulation segment is rigidly bonded to the arms forming 120° between consecutive segments, whereas the bonds between the beads forming the arms are fully flexible. The monomeric units, with diameter σ, interact through the hard-sphere intermolecular potential. The total number of segments is given by $m=1+m_1+m_2+m_3$.

It becomes clear from the ensuing discussion that it would be desirable to have a theoretical approach for branched chain molecules with the following ingredients: (1) able to clearly distinguish the structural and topological differences between the segments located along the chain arms and those forming the articulation point of the branched chain, such as the difference in flexibility; (2) simple enough to be straightforwardly applicable; (3) easy to extend for dealing with more complex systems, such as heteronuclear branched molecules and their mixtures.

The purpose of this work is threefold. First, we propose an extension of the statistical associating fluid theory, which explicitly accounts for branched chains architecture: the formation of the chain arms is calculated using the TPT1 and the articulation segments are accounted for through the TPT2. We call this version of the theory SAFT-branched (SAFT-B). Second, we use the theory to study the effect of branching on the thermodynamic properties and phase equilibria of isomeric chains. Third, we apply the proposed equation of state to predict the critical temperature of some alkanes, and results are compared with experimental data.

The rest of the paper is organized as follows: In Sec. II we describe the most relevant features of the model and theory for branched hard chains. Results and discussion are presented in Sec. III. Finally, conclusions are given in Sec. IV.

II. MOLECULAR MODEL AND THEORY

In this work we consider chainlike fluids in which molecules are modeled as m tangent hard sphere (monomers), each of diameter σ, bonded with bond length l equal to the segment diameter (see Fig. 1). The attractive interactions between the segments that form the chains are calculated

through a van der Waals mean-field Helmholtz free energy. Linear chains are described as freely jointed hard spherical units. Branched chains are modeled as molecules with three arms, each of them having m_1, m_2, and m_3 segments, respectively, and a central segment connecting them (see Fig. 1). Thus, the total chain length of a molecule, m, is given by $m=1+m_1+m_2+m_3$. This expression can be written in an equivalent way introducing m', the number of segments forming the articulation tetramer, namely, $m=m_1+m_2+m_3-3+m'$. Obviously, for $m'=4$ the previous equation is recovered, as expected. The central monomer is called the *articulation segment* or *branched point*. This segment connects the three arms of the chain with rigid bonds, forming angles of 120° between consecutive arms, as shown in Fig. 1, whereas the segments of the chain arms are jointed through fully flexible bonds.

The model, although rather crude, accounts for the most salient features of real chain molecules, such as bead connectivity (representing topological constraints and internal flexibility), the reduced mobility of segments close to the articulation point (compared to the total flexibility of the bonds located along the chain arms), to the excluded volume effects, and attractive forces between the beads forming the molecules. Because the SAFT approach is widely used in the literature, we will explain here only the most important features concerning its extension for branched chainlike molecules. For further details the reader is referred to the recent review of Müller and Gubbins.[37]

The SAFT-branched (SAFT-B) approach presented here, as other versions of SAFT, is written in terms of the Helmholtz free energy, which can be expressed as a sum of different microscopic effects: the ideal contribution, A^{ideal}, the monomer reference term, A^{mono}, that accounts for the repulsive and attractive interactions between the segments forming the chain, and the contribution due to the chain formation, A^{chain}. The Helmholtz free energy of a pure system of branched chains may be written as

$$\frac{A}{N_c k_B T}=\frac{A^{\text{ideal}}}{N_c k_B T}+\frac{A^{\text{mono}}}{N_c k_B T}+\frac{A^{\text{chain}}}{N_c k_B T}, \tag{1}$$

where N_c is the total number of molecules, T the temperature, and k_B the Boltzmann constant. Each individual contribution to the Helmholtz free energy of the system is explained separately here.

A. The ideal term

The Helmholtz free energy of an ideal system of chains can be written as follows:

$$A^{\text{ideal}}=N_c k_B T[\ln(\rho_c \Lambda^3)-1], \tag{2}$$

where $\rho_c=N_c/V$ is the chain density, V the volume, and Λ is the thermal de Broglie wavelength. The segment density of the system, ρ, is easily related to the chain density through $\rho=m\rho_c$.

B. The monomer reference term

In our case, the Helmholtz free energy corresponding to the monomer–monomer interactions consists of a sum of the contribution from the hard sphere reference fluid and that from the long-range dispersion forces

$$\frac{A^{\text{mono}}}{N_c k_B T}=\frac{A^{\text{hs}}}{N_c k_B T}+\frac{A^{\text{mf}}}{N_c k_B T}. \tag{3}$$

A^{hs}, the Helmholtz free energy of the hard sphere reference system, originally obtained by Carnahan and Starling,[41] is given by

$$A^{\text{hs}}=N_c k_B T m\,\frac{\eta(4-3\eta)}{(1-\eta)^2}. \tag{4}$$

η is the packing fraction of the hard sphere fluid, defined as

$$\eta=\frac{\pi}{6}\rho\sigma^3=\frac{\pi}{6}m\rho_c\sigma^3=m\rho_c b, \tag{5}$$

where b represents the segment volume, $b=(\pi/6)\sigma^3$.

The contribution due to the dispersive attractive interactions is given at the mean-field level in terms of the van der Waals theory,

$$A^{\text{mf}}=-N_c m\epsilon_{\text{mf}}\eta, \tag{6}$$

where ϵ_{mf} is an integrated mean-field attractive energy that accounts for the long-range dispersion forces.

C. The chain term

The Helmholtz free energy due to the chain formation can be written as

$$\frac{A^{\text{chain}}}{N_c k_B T}=\frac{A^{\text{chain}}_{\text{arm}}}{N_c k_B T}+\frac{A^{\text{chain}}_{\text{art}}}{N_c k_B T}, \tag{7}$$

where $A^{\text{chain}}_{\text{art}}$ is the Helmholtz free-energy contribution accounting for the formation of the articulation tetramer with rigid bonds described previously (see Fig. 2), and $A^{\text{chain}}_{\text{arm}}$ accounts for the free-energy contribution due to the formation of the flexible arms and their connections with the rest of the chain (central tetramer), as indicated in Fig. 2.

The contribution due to the formation of the three arms of the chain can be adequately described using the first-order perturbation contribution.[13,19] Since the chains have m_1 segments in the first arm, m_2 in the second one, and m_3 in the third one (see Figs. 1 and 2), the Helmholtz free energy given by $A^{\text{chain}}_{\text{arm}}$ can be obtained by adding each contribution associated with the individual arms, resulting the following expression:[13,19]

$$A^{\text{chain}}_{\text{arm}}=(3-m_1-m_2-m_3)\ln g_{\text{hs}}(\sigma), \tag{8}$$

which is equivalent to

$$A^{\text{chain}}_{\text{arm}}=(m'-m)N_c k_B T \ln g_{\text{hs}}(\sigma), \tag{9}$$

where $g_{\text{hs}}(\sigma)$ is the pair radial distribution function of the hard sphere fluid at the contact length. Equation (9) can be easily obtained from Eq. (8) using the relationship between m and m' introduced previously. In this work we have used the expression from Carnahan-Starling[41]

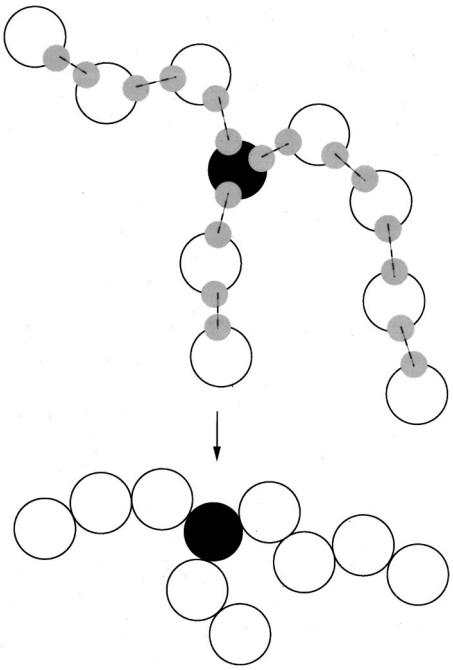

FIG. 2. Schematic representation of the formation of branched chains using Wertheim's first- and second-order perturbation theory. The blank segments are located along the chain arms (through fully flexible bonds) and the dark segment, which is rigidly bonded to the rest of the chain, represents the articulation point.

$$g_{\mathrm{hs}}(\sigma)=\frac{1-\eta/2}{(1-\eta)^3}. \tag{10}$$

$A_{\mathrm{art}}^{\mathrm{chain}}$, the Helmholtz free energy due to the formation of the articulation tetramer, is approximated in this work by

$$\frac{A_{\mathrm{art}}^{\mathrm{chain}}}{N_c k_B T}=\frac{A_{\mathrm{TPT1}}^{\mathrm{art}}}{N_c k_B T}+\frac{A_{\mathrm{TPT2}}^{\mathrm{art}}}{N_c k_B T}, \tag{11}$$

$A_{\mathrm{TPT1}}^{\mathrm{art}}$ represents the first-order perturbation term due to the formation of the tetramer and $A_{\mathrm{TPT2}}^{\mathrm{art}}$ accounts for the second-order contribution due to the formation of the articulation 4-mer molecule (see Fig. 2). Note that the most accurate perturbation order that could be used to evaluate the formation of such a molecule (4-mer chainlike) within the Wertheim's thermodynamic approach is the third order.[13,38,39] However, this term involves the hard sphere four-body distribution function for the configuration corresponding to the fully bonded molecule, as a function of the packing fraction. Unfortunately, there is neither an analytical expression nor molecular simulation data for this function from which an appropriate approximation could be developed.

The first-order contribution to the formation of the articulation tetramer, which only depends on the number of segments (in this case the number of hard sphere units is $m'=4$) and is independent of the arrangement of its monomers, is written as follows:[13,19]

$$A_{\mathrm{TPT1}}^{\mathrm{art}}=N_c k_B T(1-m')\ln g_{\mathrm{hs}}(\sigma). \tag{12}$$

$A_{\mathrm{TPT2}}^{\mathrm{art}}$ accounting for the second-order perturbation contribution due to the formation of the articulation tetramer, is given by the expression derived by Phan *et al.*,[39] which provides essentially the same thermodynamic description as the theory of Wertheim[13,38]

$$A_{\mathrm{TPT2}}^{\mathrm{art}}=-N_c k_B T\ln\left(\frac{1}{\sqrt{1+4\lambda}}\right)-N_c k_B T\ln\left[\left(\frac{1+\sqrt{1+4\lambda}}{2}\right)^{m'}-\left(\frac{1-\sqrt{1+4\lambda}}{2}\right)^{m'}\right], \tag{13}$$

where λ is a new parameter introduced in the theory that depends on the packing fraction and molecular geometry. Although Eq. (13) accounts for the formation of the articulation tetramer at the second-order perturbation level, this version of the theory does not contain explicitly the geometry of the articulation point, but only its rigidity and the number of segments forming the tetramer. Since this articulation point is associated with four monomeric segments, we have set $m'=4$ in Eq. (13). Phan *et al.*[39] have demonstrated that the previous equation may be expressed in a simplified way if $\lambda \ll 1$. In this case $(1-\sqrt{1+4\lambda})/(1+\sqrt{1+4\lambda})$ is also small compared to unity, and Eq. (13) may be written as[39]

$$A_{\mathrm{TPT2}}^{\mathrm{art}}=-N_c k_B T\ln\left\{\frac{(1+\sqrt{1+4\lambda})^{m'}}{2^{m'}\sqrt{1+4\lambda}}\right\}. \tag{14}$$

Equations (13) and (14) are valid for flexible and rigid molecules. Note that $m'=4$ in Eq. (14), as in the previous one, and the only difference between both equations arises from a different dependence with λ. If the bonds that form the tetramer are rigid, λ is given by[13,38,39]

$$\lambda=\frac{g_{\mathrm{hs}}^{(3)}(\sigma,\sigma,u)}{[g_{\mathrm{hs}}(\sigma)]^2}-1, \tag{15}$$

where u is a function defined as $u=2\sigma\sin(\omega/2)$, where ω is the bond angle, and $g_{\mathrm{hs}}^{(3)}(\sigma,\sigma,u)$ is the three-body distribution function of three tangentially hard sphere segments with end segments forming an angle ω.

In order to obtain the most reliable description of the thermodynamic properties, accurate values of the hard sphere three-body distribution function at the contact geometry, as a function of the packing fraction, are needed. Attard and Stell[42] have obtained an expression for $g_{\mathrm{hs}}^{(3)}(\sigma,\sigma,u)$ using the Percus–Yevick closure relation to solve the Ornstein–Zernike integral equation (triplet approximation, PY3)[43]

$$g_{\mathrm{hs}}^{(3)}(\sigma,\sigma,u)=g_{\mathrm{hs}}(\sigma)g_{\mathrm{hs}}(\sigma)g_0(\sigma,\sigma,u), \tag{16}$$

where g_0 is a new hard sphere three-body distribution function defined by the previous equation. Müller and Gubbins[38] have used these results and proposed an analytical functional form for g_0, which depends on the packing fraction,

$$g_0=\frac{1+a\,\eta+b\,\eta^2}{(1-\eta)^3}, \tag{17}$$

where a and b are angle-dependent constants. Values of a and b can be found in the Appendix of the work from Müller

and Gubbins.[38] Molecular simulation results obtained by Attard[43] and Müller and Gubbins[44] show that the PY3 approximation accurately describes the behavior of g_0 in a wide range of densities ($0 \leqslant \eta \leqslant 0.47$), including the limit of high packing fractions.

To recap, the Helmholtz free energy due to the formation of branched chains formed by m segments and n_{art} articulation points can be easily written as

$$A^{\mathrm{chain}} = N_c k_B T (1-m) \ln g_{\mathrm{hs}}(\sigma) - N_c k_B T n_{\mathrm{art}} \ln \left\{ \frac{(1+\sqrt{1+4\lambda})^{m'}}{2^{m'}\sqrt{1+4\lambda}} \right\}, \tag{18}$$

where we have assumed that each of the n_{art} articulation tetrames contributes equally to the Helmholtz free energy. Since the Helmholtz free energy depends only on m, m', and n_{art}, and the second parameter (m') is kept fixed for the isomers considered in this work, SAFT-B predicts identical thermodynamic properties for branched molecules with the same number of segments and articulation points.

To describe real branched molecules we have used the model and theory presented here under the united atoms model approach.[22,30,37] Alkanes are modeled as homonuclear chainlike molecules with fixed bond length. Different chemical groups, such as CH_3, CH_2, and CH, are described as hard spherical segments with the same diameter, interacting through a mean-field attractive force at the van der Waals level. A simple empirical relationship, introduced by Jackson and Gubbins,[45] between the number of carbon atoms C in the alkane molecule and the number of spherical segments is used to calculate the chain length, which is given by $m = 1 + (C-1)/3$. This equation, which gives a reasonable description of the critical temperatures of the homologous series of *n*-alkanes, is also used in this work to describe branched alkanes. Since the critical temperature of alkanes mainly depends on the number of carbon atoms, we expect this approximation to be appropriate in the framework of this work. To be consistent with the election of m, m' is calculated according to the same rule, namely $m' = 1 + (C' - 1)/3$, where C' is the number of carbon atoms in the articulation tetramer. Since real branched chains with three arms are formed by four carbon atoms, m' is set equal to 2. This value is used to describe all the alkane isomers considered in this work. Note that the value chosen for m' should be understood as an *effective* way to account for the effect of the branching degree on the thermodynamic behavior of a given system. An equivalent way to calculate the value of m' is as follows. Consider the unique branched alkane formed by four carbon atoms, 2-methylpropane. In this special case, the total number of segments is equal to the number of beads forming the articulation tetramer, and hence $m = m'$. When a heavier three-arm alkane is considered, the value of m increases according to the empirical rule of Jackson and Gubbins,[45] whereas the value of m' is kept constant and equal to 2.

III. RESULTS AND DISCUSSION

We apply the SAFT-B approach outlined in the previous section to study the thermodynamic properties and vapor–liquid equilibria for linear and branched chainlike fluids. We first study the compressibility factor, $Z = P/\rho_c k_B T$, of isomeric chains, and investigate the effect of branching on pressure. We next consider the phase equilibria of branched chains of several isomers and its comparison with that corresponding for linear molecules. Finally, we compare the predicted critical temperatures for some alkanes with experimental data taken from the literature in order to assess the accuracy of the SAFT-B approach.

To obtain the coexistence curve of pure fluids, we have determined the vapor–liquid equilibrium properties by solving the equilibrium conditions

$$P_L(\eta_L, T) = P_V(\eta_V, T), \tag{19}$$

$$\mu_L(\eta_L, T) = \mu_V(\eta_V, T), \tag{20}$$

where the subscripts refer to the liquid (L) and vapor (V) phases. For simplicity, the integrated mean-field energy, ϵ_{mf}, will be considered here as the unit of energy and the hard sphere diameter, σ, as the unit of length. Hence, the reduced temperature is defined as $T^* = k_B T/\epsilon_{\mathrm{mf}}$ and the reduced pressure as $P^* = Pb/\epsilon_{\mathrm{mf}}$, where b is the monomer volume previously defined in Sec. II.

A. Thermodynamic properties and phase equilibria of branched chains

In this section we consider athermal branched chains, i.e., systems in which the intermolecular potential between the molecules is purely repulsive and no mean-field attractive contribution to the Helmholtz free energy is considered. This can be obtained from the theory outlined in the previous section by setting the free energy associated with the mean-field contribution equal to zero, $A^{\mathrm{mf}} = 0$, in Eq. (3).

We first study chainlike molecules formed by four and five hard spherical segments. Figure 3 shows a schematic two-dimensional view of some isomers considered here and described by the SAFT-B approach, classified by the number of segments and articulation points per molecule. We have only shown the chain models for which SAFT-B predicts different thermodynamic properties. Other isomers, such as a system formed by chains with six segments ($m = 6$) and one articulation point occupying the third position in the main backbone of the chain, have identical thermodynamic properties (predicted by SAFT-B) as systems with the same number of segments and articulation points per molecule. This is a direct consequence of the approximations used to derive the equation of state presented in this work.

Figure 4(a) shows the compressibility factor, as a function of the packing fraction, of four different hard chains. Curves corresponding to low compressibility factor values represent the predictions for isomeric molecules with four segments ($m = 4$) and those for high compressibility values to chains with $m = 5$. In both cases, solid lines represent the predictions corresponding to linear chains and dashed lines are the results for branched molecules with one articulation point. SAFT-B predicts similar pressure values for different

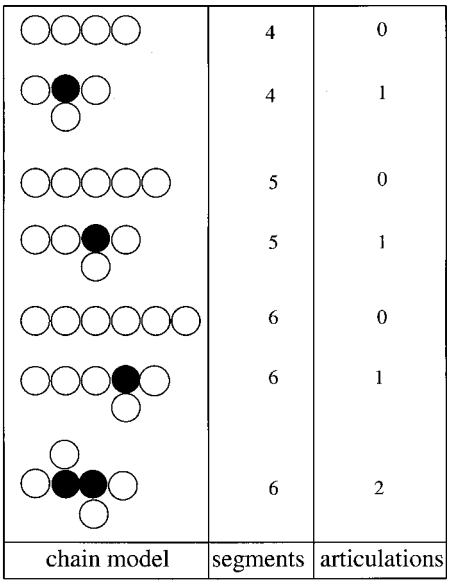

FIG. 3. A representation of some of the isomers considered by the SAFT-B equation of state with four, five, and six hard-sphere segments.

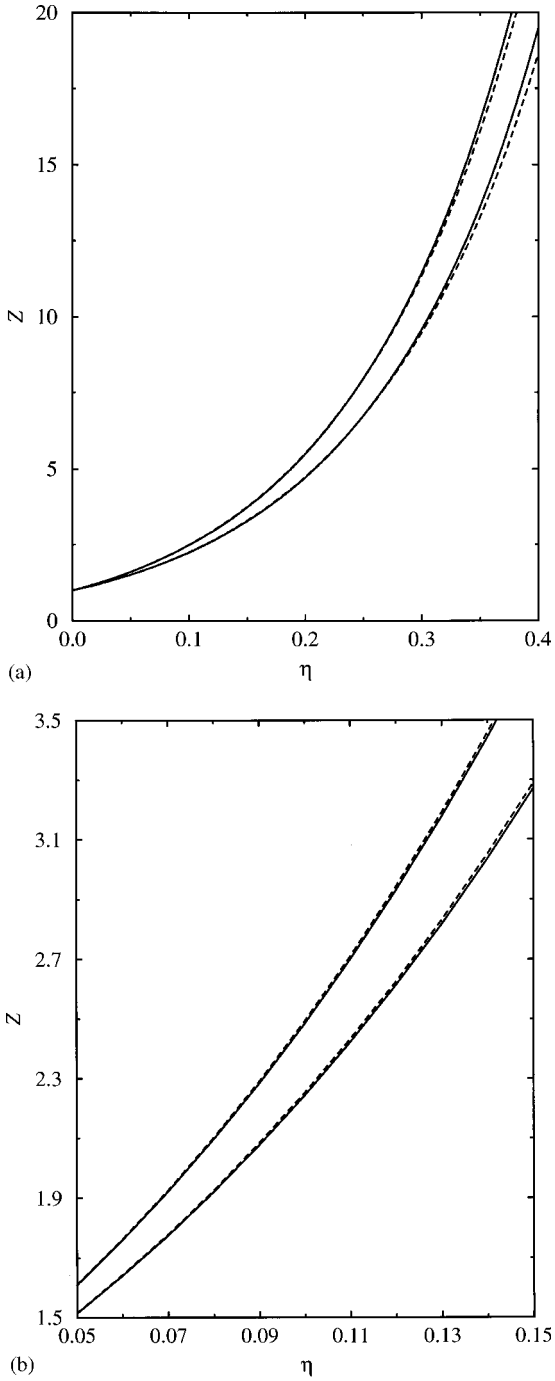

FIG. 4. Compressibility factor, as a function of the packing fraction, of linear and branched hard chains: (a) in the whole fluid range; (b) enlargement of the low packing fraction region. Solid lines represents the predictions for linear chains and dashed lines are those corresponding to branched chains with one articulation point for molecules formed by four (lower curves) and five (upper curves) segments.

chains (at a given chain length and packing fraction), although the compressibility factor of branched molecules, as a function of packing fraction, exhibits a different curvature than that for linear chains. Due to this, the pressure of branched hard molecules is lower than the corresponding for linear isomers at high packing fractions, but higher at low and intermediate densities. This behavior, which can be observed more clearly in Fig. 4(b), seems indeed reasonable since the excluded volume, and hence the pressure, are expected to increase with the stiffness, because it is harder to pack less flexible molecules. The same general trend is also observed when Monte Carlo simulation results from Müller and Gubbins[38] for a branched tetramer are compared to simulation data from Dickman and Hall[46] corresponding to linear chains. Finally, note that this prediction is in agreement with previous results obtained from Phan *et al.*,[39] who compared the compressibility factor of freely jointed and freely rotating chains. These authors have found that the pressure of less flexible molecules is slightly larger than the pressure of freely jointed chains at the low and intermediate density range.

It is also observed that the difference between the pressure corresponding to linear and branched chains, at the same packing fraction, decreases with the chain length. This has also been observed by other authors,[14,15] and it is expected, since the pressure of repulsive chain systems is not a strong function of the details of the molecular structure; it mainly depends on the number of segments per chain. As the chain length is increased, the relative number of beads close to the articulation point decreases. This effect is qualitatively described by the SAFT-B approach: The Helmholtz free energy that accounts for the branching effect is essentially independent of *m*, whereas the free-energy contribution due to the formation of the chain arms scales with the number of segments.

We have also studied the behavior of the compressibility factor versus the packing fraction of some isomers corresponding to molecules with 6, 10, and 16 segments (see the schematic two-dimensional view for some molecular models in Fig. 3). Different curves in Fig. 5(a) represent the compressibility factor of systems formed by hard chains with six (lowest compressibility values) and ten segments (higher compressibility factors), and different number of articulation points per molecule: one (dotted lines), two (long-dashed lines), three (long-dashed line), and four (dot-dashed line). Solid lines represent the theoretical compressibility of linear

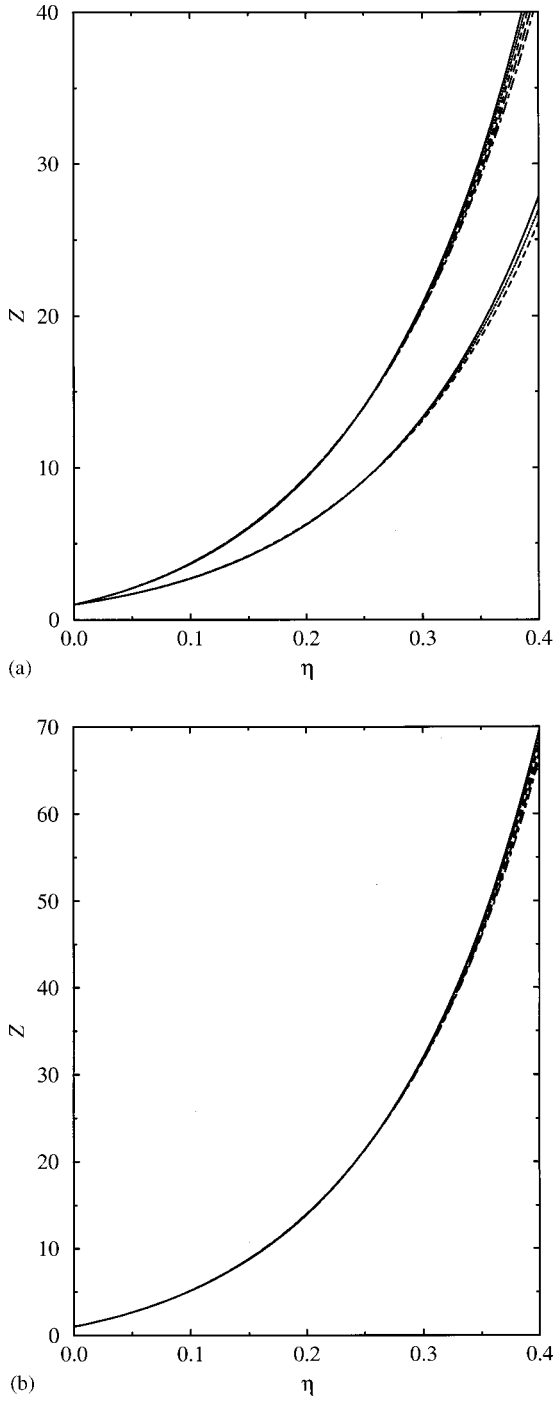

FIG. 5. Compressibility factor, as a function of the packing fraction, of linear and branched hard chains with (a) six, ten, and (b) sixteen segments. Solid lines (linear), dotted lines (one articulation point), dashed lines (two articulation segments), long-dashed line (three articulation points), and dot-dashed line (four articulation beads) represent the theoretical predictions for chainlike isomeric molecules obtained from SAFT-B.

chains. Two main effects are observed: First, the compressibility factor of the system is increased as the chain length is larger, and second, the compressibility factor corresponding to branched chains decreases as the branching degree is higher. We have also considered longer linear and branched hard chain molecules ($m=16$) with one, two, three, and four articulation points [Fig. 5(b)]. As can be observed, the same general trend is found for longer molecules as the branching

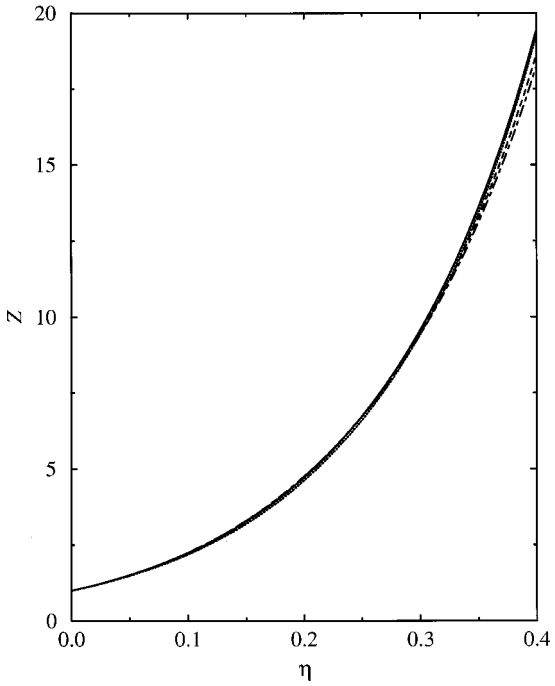

FIG. 6. Compressibility factor, as a function of the packing fraction, of linear and branched tetramers. Solid and dotted lines represent the predictions from TPT1 and TPT2, respectively, for linear tetramers, and dashed and dot-dashed lines are those corresponding to branched tetramers using SAFT-B and TPT2 for starlike molecules, respectively.

degree of the system is increased. Although it is not shown here, the SAFT-B equation of state also predicts a compressibility factor-packing fraction curve with different shape or curvature for linear and branched chains, as in previous systems.

Before presenting the results corresponding to the vapor–liquid phase behavior of branched chains, we have analyzed the effect of branching for both linear and branched molecules, treated at the same perturbation level, namely TPT2. This comparison is important since TPT1 does not distinguish between linear and branched chains. The simplest case in which the implementation of the TPT2 approach for two isomeric molecules can be easily done is that for chains formed by four segments. We have used the two TPT2 versions introduced by Phan *et al.*[39] to describe the thermodynamic behavior of both systems. Figure 6 shows the compressibility factor, as a function of packing fraction, of these fluids. For comparison, we have also included the results for a linear tetramer using TPT1, as well as the predictions obtained from SAFT-B corresponding to the branched isomer. As can be seen, TPT1 and TPT2 predict similar values and curvature for the compressibility factor of linear chains in the whole range of densities. The TPT2 version of Phan *et al.* for starlike molecules [see Eq. (36) in Ref. 39, with $m=1$ and $f=3$] predicts a compressibility factor for branched chains lower than that for linear isomers at high densities, but higher at low and intermediate packing fractions. This means that the TPT2 approach also predicts a crossing region in the compressibility factor curves of linear and branched tetramers at low densities, in agreement with results obtained from SAFT-B. Some deviations between both theories (TPT2 for

starlike molecules and SAFT-B) are observed at high densities, due to the fact that the TPT2 theory accounts explicitly for the geometry of this kind of fluid, whereas the SAFT-B equation of state only describes its rigidity and the number of segments in the articulation tetramer. The great advantage of SAFT-B over a more standard TPT2 version, such as the TPT2 approaches of Wertheim[13] and Phan *et al.*,[39] is that it can be easily used to describe the thermodynamic behavior of branched chains with $m>4$.

In summary, the main effect of branching degree on the thermodynamic properties of hard chain fluids is to decrease the compressibility factor of the system at high densities. On the contrary, the pressure of branched molecules is higher than that of linear chains at low and intermediate packing fractions. The difference between the pressure values corresponding to different isomers increases as the packing fraction is higher and decreases as the chain length increases.

We next proceed to investigate the vapor–liquid properties of some branched chains with attractive interactions at the mean-field level of van der Waals. Figure 7(a) shows the coexistence diagram of four different molecules, two linear (solid lines), and two branched chains with one articulation point (dashed lines). The molecular architecture of these molecules is shown in Fig. 3. The coexisting curves at low temperatures correspond to isomeric molecules formed by four segments and those at higher temperatures to isomers with five beads. In this figure we have only considered the upper region of the vapor–liquid phase diagram of the systems studied, where the differences between the coexisting properties are larger. As can be observed, the main effect of the presence of one articulation point in the chain on the upper region of the coexistence diagram is to decrease the critical temperature and density with respect to the corresponding values for linear isomers. This behavior, predicted by the SAFT-B equation of state, which is also observed in real systems such as branched alkanes of low molecular weight,[47] can be explained by taking into account the results obtained for the compressibility factor of linear and branched chains. Since the mean-field free-energy contribution at a given packing fraction is the same for any isomer, the differences between the phase behavior of both systems can be attributed to the difference in the equation of state corresponding to the hard sphere reference fluid. In particular, the lower value of the critical temperature of branched chains (compared to that of linear molecules) is a direct consequence of a higher value for the compressibility factor of branched chains with respect to that of linear molecules at low densities.

We have also analyzed the liquid phase envelope of isomers with four and five segments at low temperatures. As can be seen in Fig. 7(b), a crossing region exists in the liquid branch between linear and branched molecules around $\eta \sim 0.245$, which is consistent with the crossing observed in the compressibility factor between isomeric molecules.

Finally, we consider the effect of the number of articulation points per molecule on the phase behavior. The vapor–liquid coexistence curves of three isomers formed by six segments are shown in Fig. 8. The solid line represents the vapor–liquid equilibria of linear chains, the dashed line that

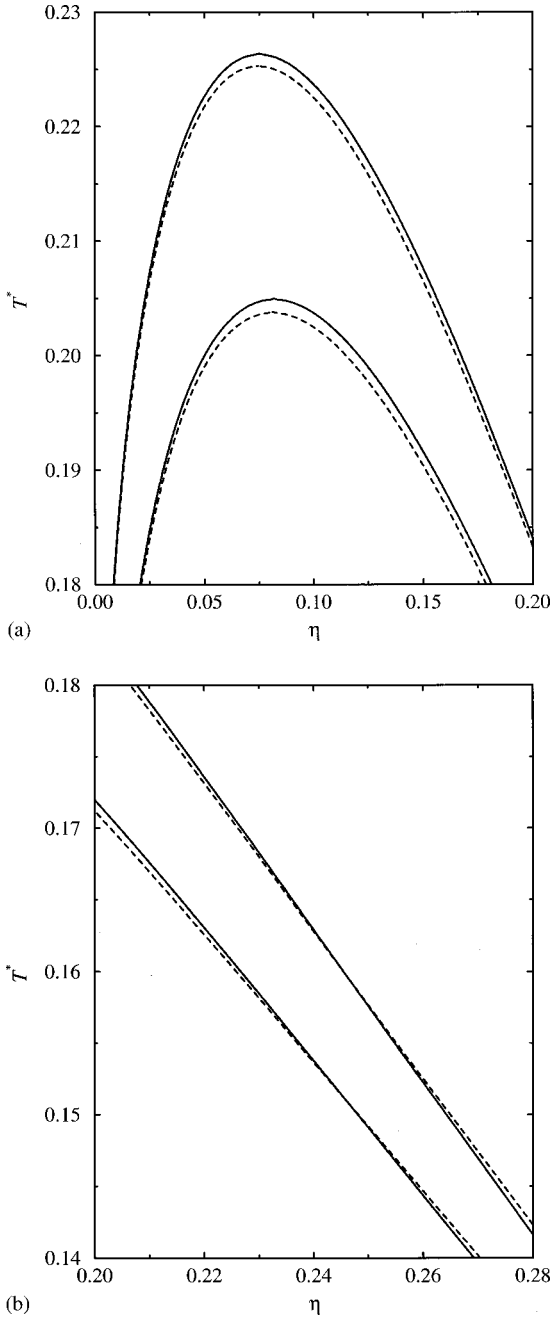

FIG. 7. Vapor–liquid coexisting curve of hard chains with attractive interactions at the van der Waals level: (a) upper region of the diagram; (b) enlargement of the phase diagram corresponding to the liquid branch at low temperatures. Lines represent the theoretical predictions for linear chains (solid lines) and branched molecules with one articulation point (dashed lines) formed by four (lower curves) and five (upper curves) segments.

of branched molecules with one articulation point, and the long-dashed line corresponds to branched isomeric molecules with two articulation segments. As in the previous systems, the effect of branching on the phase diagram is to shift the coexistence curve to lower temperatures and densities. This displacement increases as the number of articulation points in the molecule is increased.

Summarizing, the main effect of branching on the phase behavior of fluids formed by branched chains which interact through a mean-field attractive potential at the level of van der Waals is to shift the vapor–liquid coexistence curve to

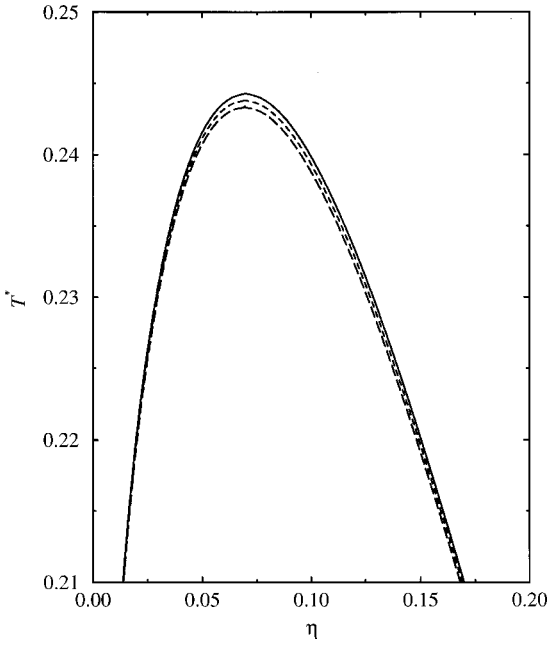

FIG. 8. Vapor–liquid coexistence diagram for hard chains with attractive interactions at the van der Waals level. Solid lines (linear), dashed lines (one articulation point), and long-dashed lines (two articulation segments) are the theoretical predictions for chainlike molecules formed by six segments.

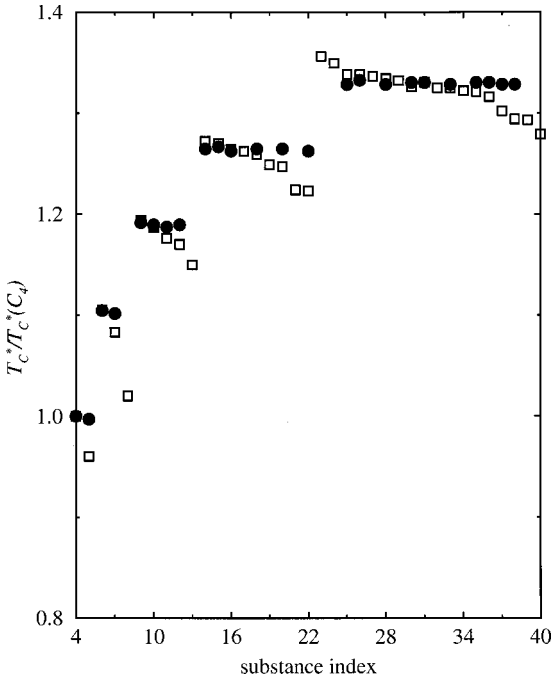

FIG. 9. Critical temperatures (reduced with respect to the critical temperature of *n*-butane) of alkanes up to eight carbon atoms. Squares correspond to the experimental data taken from the literature (Ref. 47), and dark circles represent the predictions obtained from the SAFT-B equation of state. Each alkane is represented by an integer number along the *x* axis which is shown in Table III of (Ref. 48).

lower temperatures and densities as the branching degree is made larger.

B. Critical temperatures of *n*-alkane isomers

The molecular models studied in the previous section can be used to understand the phase behavior of real systems, such as branched alkanes. These substances have different coexistence envelopes and critical properties than those corresponding to linear alkanes.[47]

Figure 9 shows the critical temperatures (reduced with respect to the experimental critical temperature of *n*-butane) of linear and branched alkanes up to eight carbon atoms. We use the critical temperature of *n*-butane as unit of temperature because this molecule can be considered as the first *n*-alkane that shows a regular behavior with respect to the rest of the members of the homologous series. For each group of isomers, the experimental critical temperature of a given alkane in that group is plotted in order of decreasing temperature, and the corresponding prediction from the SAFT-B is represented for the same value of the *x* axis. This way of representing the critical temperatures of alkanes has been introduced previously by MacDowell and Vega.[48] In order to identify which particular alkane corresponds to each integer number in the *x* axis, MacDowell and Vega have represented in a table (see Table III of their work) a list of the alkanes considered together with the substance index used to represent it. Squares correspond to the experimental data taken from the literature[47] and circles represent the predictions from the theory. As can be observed, SAFT-B quantitatively describes the critical temperature of *n*-alkane molecules. However, agreement between experimental results and predictions from the SAFT-B equation of state is only qualitative for branched alkanes. This behavior is expected since the proposed molecular model is rather crude to describe the finer differences between isomeric alkanes. The model only takes into account the fact that the adjacent segments to the articulation point are rigidly bonded to the chain arms, while those forming the rest of the chain (arms of the molecule) are freely jointed.

The theoretical predictions could be improved by introducing some modifications in the model and theory. It is possible to consider a more realistic model in which branched chains are represented by heteronuclear chains, i.e., the segments modeling the chemical groups of alkane molecules can have different molecular parameters. This modification in the model, which introduces different molecular volumes in the description of linear and branched chains, has proven to be important in previous studies of isomeric molecules.[48] A further modification in the model consists of including a more accurate description of the dispersive (attractive) intermolecular forces. As discussed by Yethiraj and Hall[14] and Escobedo and de Pablo,[15] the effect of branching on the thermodynamic properties of the system will be more pronounced for molecules with attractive interactions, such as the Lennard-Jones intermolecular potential. Unfortunately, there is no analytical expression available at present for the three-body correlation function of the reference fluid (as a function of the reduced temperature and density).

IV. CONCLUSIONS

We have presented an extension of the statistical associating fluid theory to describe branched chainlike molecules. The so-called SAFT-Branched (SAFT-B) equation of state is

based on Wertheim's first- and second-order thermodynamic perturbation theory for chain fluids. The branched chains, formed by three arms of hard spherical segments bonded through fully flexible bonds, are described at the first-order perturbation level, and the articulation points, modeled by rigid bonds forming 120°, are considered using the second-order perturbation approach.

The results obtained show that the SAFT-B equation of state qualitatively predicts the general trends of the model: The pressure of a branched hard chain is lower than that corresponding to a linear molecule with the same number of segments at high densities, but higher at low and intermediate packing fractions. We have also investigated the vapor–liquid equilibria of isomeric molecules. SAFT-B predicts a shift towards lower temperatures and densities with respect to those corresponding to linear chains, in qualitative agreement with experimental data.

To verify if SAFT-B captures the real features of isomeric molecules, we have studied the critical temperature of light branched alkanes. The results show that the theory qualitatively predicts the available experimental data, although the proposed molecular description is too simple to account for the finer details of the molecular architecture of branched chains. The great advantage of the theory proposed in this work is that it can be easily applied to other reference fluids, if their structural properties are known.

ACKNOWLEDGMENTS

This work was supported by the Spanish Government under Project No. PB96-1025 and VI Plan Propio de Investigación de la Universidad de Huelva. One of the authors (F.J.B.) acknowledges a doctoral fellowship from Comisionat per a Universitats i Recerca from the Generalitat de Catalunya during the course of this work.

[1] *Equations of State for Fluids and Fluid Mixtures*, edited by J. V. Sengers, R. F. Kayser, C. J. Peters, and H. J. White, Jr. (Elsevier, Amsterdam, 2000).
[2] D. Chandler and H. C. Handersen, J. Chem. Phys. **57**, 1930 (1973).
[3] D. Chandler, J. Chem. Phys. **59**, 2742 (1973).
[4] K. S. Schweizer and J. G. Curro, Phys. Rev. Lett. **58**, 246 (1987).
[5] J. G. Curro and K. S. Schweizer, Macromolecules **20**, 1928 (1987).
[6] J. G. Curro and K. S. Schweizer, Macromolecules **21**, 3070 (1988); *ibid.* **21**, 3082 (1988).
[7] K. G. Honnell, J. G. Curro, and K. S. Schweizer, Macromolecules **23**, 3496 (1990).
[8] M. D. Donohue and J. M. Prausnitz, AIChE J. **24**, 849 (1978).
[9] R. Dickman and C. K. Hall, J. Chem. Phys. **85**, 4108 (1986).
[10] K. G. Honnell and C. K. Hall, J. Chem. Phys. **90**, 1841 (1989).
[11] Y. C. Chiew, Mol. Phys. **70**, 129 (1990).
[12] M. S. Wertheim, J. Stat. Phys. **35**, 19 (1984); *ibid.* **35**, 35 (1984); *ibid.* **42**, 459 (1986); *ibid.* **42**, 477 (1986).
[13] M. S. Wertheim, J. Chem. Phys. **87**, 7323 (1987).
[14] A. Yethiraj and C. K. Hall, J. Chem. Phys. **94**, 3943 (1991).
[15] F. A. Escobedo and J. J. de Pablo, J. Chem. Phys. **103**, 1946 (1995).
[16] W. G. Chapman, K. E. Gubbins, G. Jackson, and M. Radosz, Fluid Phase Equilibria **52**, 31 (1989).
[17] W. G. Chapman, K. E. Gubbins, G. Jackson, and M. Radosz, Ind. Eng. Chem. Res. **29**, 1709 (1990).
[18] G. Jackson, W. G. Chapman, and K. E. Gubbins, Mol. Phys. **65**, 1 (1988).
[19] W. G. Chapman, G. Jackson, and K. E. Gubbins, Mol. Phys. **65**, 1057 (1988).
[20] S. H. Huang and M. Radosz, Ind. Eng. Chem. Res. **29**, 2284 (1990).
[21] S. H. Huang and M. Radosz, Ind. Eng. Chem. Res. **30**, 1994 (1991).
[22] A. Galindo, P. J. Whitehead, G. Jackson, and A. N. Burgess, J. Phys. Chem. **100**, 6781 (1996).
[23] W. G. Chapman, J. Chem. Phys. **93**, 4299 (1990).
[24] J. K. Johnson, E. A. Müller, and K. E. Gubbins, J. Phys. Chem. **98**, 6413 (1994).
[25] E. A. Müller, L. F. Vega, and K. E. Gubbins, Mol. Phys. **86**, 1209 (1994).
[26] A. Gil-Villegas, A. Galindo, P. J. Whitehead, S. J. Mills, G. Jackson, and A. N. Burgess, J. Chem. Phys. **106**, 4168 (1997).
[27] A. Galindo, L. A. Davies, A. Gil-Villegas, and G. Jackson, Mol. Phys. **93**, 241 (1998).
[28] C. McCabe and G. Jackson, Phys. Chem. Chem. Phys. **1**, 2057 (1999).
[29] F. J. Blas and L. F. Vega, Mol. Phys. **92**, 135 (1997).
[30] F. J. Blas and L. F. Vega, Ind. Eng. Chem. Res. **37**, 660 (1998).
[31] F. J. Blas and L. F. Vega, J. Chem. Phys. **109**, 7405 (1998).
[32] L. F. Vega and F. J. Blas, Fluid Phase Equilibria **171**, 91 (2000).
[33] F. J. Blas, O. R. Contreras, A. D. Mackie, and L. F. Vega, J. Chem. Phys. (in press).
[34] E. J. M. Filipe, E. J. S. Gomes de Azebedo, L. F. G. Martins, V. A. M. Soares, J. C. G. Calado, C. McCabe, and G. Jackson, J. Phys. Chem. B **104**, 1315 (2000).
[35] E. J. M. Filipe, L. F. G. Martins, J. C. G. Calado, C. McCabe, and G. Jackson, J. Phys. Chem. B **104**, 1322 (2000).
[36] F. J. Blas, J. Phys. Chem. B **104**, 9239 (2000).
[37] E. A. Müller and K. E. Gubbins, in *Associating Fluids and Fluid Mixtures*, edited by J. V. Sengers, R. K. Kayser, C. J. Peters, and H. J. White (Elsevier, Amsterdam, 2000).
[38] E. A. Müller and K. E. Gubbins, Mol. Phys. **80**, 957 (1993).
[39] S. Phan, E. Kierlik, M. L. Rosinberg, H. Yu, and G. Stell, J. Chem. Phys. **99**, 5326 (1993).
[40] K. P. Shukla and W. G. Chapman, Mol. Phys. **98**, 2045 (2000).
[41] N. F. Carnahan and K. E. Starling, J. Chem. Phys. **51**, 635 (1969).
[42] P. Attard and G. Stell, Chem. Phys. Lett. **189**, 128 (1992).
[43] P. Attard, J. Chem. Phys. **91**, 3072 (1989).
[44] E. A. Müller and K. E. Gubbins, Mol. Phys. **80**, 65 (1993).
[45] G. Jackson and K. E. Gubbins, Pure Appl. Chem. **61**, 1021 (1989).
[46] R. Dickmann and C. K. Hall, J. Chem. Phys. **89**, 3168 (1988).
[47] B. D. Smith and R. Srivastava, *Thermodynamic Data for Pure Compounds* (Elsevier, London, 1986).
[48] L. G. MacDowell and C. Vega, J. Chem. Phys. **109**, 5681 (1998).